Curvilinear coordinate formulation for vibration–rotation–large amplitude internal motion interactions. II. Application to the water molecule

Yuhua Guan and C. Richard Quade

Articles you may be interested in

A reaction-path Hamiltonian described with quasirectilinear vibrational coordinates constructed from a nonlinear combination of curvilinear internal coordinates: Formulation
J. Chem. Phys. 113, 3130 (2000); 10.1063/1.1287278

Curvilinear coordinate formulation for vibration–rotation–large amplitude internal motion interactions. I. The general theory
J. Chem. Phys. 84, 5624 (1986); 10.1063/1.449923

Internal coordinate formulation for the vibration-rotation energies of polyatomic molecules. II. Symmetric top molecules with a threefold axis
J. Chem. Phys. 80, 3528 (1984); 10.1063/1.447197

The interaction of a large amplitude internal motion with other vibrations in molecules. The effective Hamiltonian for the large amplitude motion
J. Chem. Phys. 65, 700 (1976); 10.1063/1.433084

Internal coordinate formulation for the vibration–rotation energies of polyatomic molecules
J. Chem. Phys. 64, 2783 (1976); 10.1063/1.432577

Curvilinear coordinate formulation for vibration–rotation–large amplitude internal motion interactions. II. Application to the water molecule[a]

Yuhua Guan[b] and C. Richard Quade

Department of Physics, Texas Tech University, Lubbock, Texas 79409

The vibration–rotation–large amplitude internal motion (LAM) interaction theory developed in the previous paper, hereby referred to as I, is now applied to calculate the vibration–rotation energy levels of the water molecule treating the bending mode as the LAM. Fourier sine functions are used as the basis for the bending mode, harmonic oscillator functions for the two stretching modes, and Wang functions for the rotational motion. Using the Hoy–Mills–Strey (HMS) and Hoy–Bunker (HB) force constants and molecular geometry, the vibration–rotation–LAM energy levels have been calculated from $n_\tau = 0$ to 2 for the bending mode and from $J = 0$ to 10 for the rotational motion, as well as for the first excited states of the stretching modes. A revised set of force constants, referred to as the Guan–Quade (GQ) force constants, have been determined which fit the vibrational data substantially better and fit the rotational data in some cases better and in all respects at least as well as the HB force constants. In all cases the GQ and HB force constants give a better fit to the observed rotational data than the HMS force constants.

I. INTRODUCTION

Calculation of vibration–rotation energy levels for the water molecule has been of interest for a long time. Different theories have been applied to approach the problem. Hoy, Mills, and Strey[1] and Quade[2] formulated the vibration–rotation theory in different ways treating all vibrations as small amplitude. The theory was applied to the water molecule to calculate the spectroscopic coefficients ω_k, $\chi_{kk'}$, α_k^i, etc. Hougen, Bunker, and Johns[3] formulated a vibration–rotation–bending theory for triatomic molecules. Based on this theory, Bunker and co-workers[4] developed several different models for the H_2O molecule to solve the Schrödinger equation numerically to obtain the bending–rotation energy levels. Whitehead and Handy,[5] and Maessen, Wolfsberg, and Chen[6] have applied a variational theory to H_2O to calculate the vibration–rotation energy levels.

In a previous paper[7] which is referred to as I, we developed a vibration–rotation–large amplitude internal motion interaction theory. In the theory curvilinear coordinates were used for all of the internal motions. An internal coordinate transformation, the R transformation, and an external coordinate axis rotation, the T transformation, were combined to delete the vibration–rotation coupling and the vibration–LAM coupling in zeroth order of the series expansion in the vibrational coordinates. A Van Vleck perturbation approach was used to obtain the effective rotation–LAM Hamiltonian, $H_{\tau R}^{\mathrm{eff}}$, for the molecule in the nth vibrational state, where τ denotes the large amplitude coordinate and R denotes three external rotational coordinates. Equation (69) of I gives the effective rotation–LAM

Hamiltonian as

$$H_{\tau R}^{\mathrm{eff}} = H_\tau^0 + H_\tau' + \Sigma H_{\tau,k}'(n_k + 1/2)$$
$$+ H_R^0 + H_R' + \Sigma H_{R,k}'(n_k + 1/2)$$
$$+ H_{\tau R}^0 + H_{\tau R}' + \Sigma H_{\tau R,k}'(n_k + 1/2) + H_{\mathrm{CD}} . \quad (1)$$

In the notation, k denotes the $3N - 7$ normal coordinates for the small vibrations and n_k is the vibrational quantum number of the kth normal coordinate. All H^0 terms are completely independent of the $3N - 7$ vibrations. The H' terms have their origin in the interaction with the $3N - 7$ vibrations. H_{CD} is the rotational centrifugal distortion and has the same form as in previous calculations.[8] All terms in $H_{\tau R}^{\mathrm{eff}}$ can depend explicitly upon τ. Equations (70)–(76) of I show the details of $H_{\tau R}^{\mathrm{eff}}$.

To calculate the vibrational transition frequencies, the vibrational energy has to be considered together with $H_{\tau R}^{\mathrm{eff}}$. From Eq. (77) of I, the vibrational energy is given by the usual expression:

$$\mathscr{E}_v = \Sigma \omega_k (n_k + 1/2) + \Sigma \chi_{kk'} (n_k + 1/2)(n_{k'} + 1/2) ,$$
$$(2)$$

where the ω_k are the kth harmonic vibrational frequencies independent of τ while the $\chi_{kk'}$ depend explicitly upon τ. It is direct to show that the $\chi_{kk'}$ have the same form as Eqs. (40)–(41) of Ref. 2, while the anharmonic force constants and the G-matrix elements in the $\chi_{kk'}$, i.e., f_{kkk}, $g_{kk,k}$, etc., are of different form in the present equations because of the R transformation and the resultant different normal coordinate transformations.

In this paper the general theory developed in I is applied to the H_2O molecule to calculate the vibration–rotation–LAM energy levels. The bending mode is treated as a LAM. Two different sets of force constants and molecular geometry, which were determined by Hoy–Mills–Strey[1] and Hoy–Bunker,[4(d)] are used separately. In Sec. II the effective

Hamiltonian of the H_2O molecule is introduced in detail. In Sec. III the basis functions and the calculation procedure are discussed. In Secs. IV and V the calculated vibration–rotation–LAM energy levels from a computer solution are reported.

II. THE EFFECTIVE VIBRATION–ROTATION–LAM HAMILTONIAN FOR THE H_2O MOLECULE

In this section the procedure discussed in I for obtaining the effective Hamiltonian is applied to the H_2O molecule. The molecular configuration and coordinate system are shown in Fig. 1. The supplementary bending angle τ is treated as the large amplitude coordinate (LAC). The small vibrational coordinates are characterized by the two bond stretching modes, S_+ and S_-, in a symmetry coordinate basis. A molecular axis system is established where the y axis coincides with the bisector of the bending angle and the y–z plane is taken as the molecular plane. Based on this coordinate system, the kinetic energy coefficients are calculated as a power series expansion in S_+ and S_- in velocity space. All coefficients depend explicitly upon the LAC, τ, which is defined to be supplementary to the bending angle θ for H_2O for convenience of solution. The molecular axis system is the principal axis system for the zeroth order of the inertia tensor.

According to the general theory, the R transformation is applied to delete the zeroth order vibration–LAM interactions. For the H_2O molecule, $(G_{\tau+}^{-1})^0$ is the only nonzero, zeroth order vibration–LAM interaction kinetic energy coefficient. Therefore the only nonzero R-transformation coefficient, from Eq. (9) of I, is $R_{\tau+}$. The R transformation yields the new LAC,

$$\tau' = \tau + R_{\tau+} S_+ , \tag{3}$$

with the transformation coefficient given by

$$R_{\tau+} = -\sqrt{2}\eta(\sin \tau)^{-1} l^{-1}(1 - \eta - \eta \cos \tau) , \tag{4}$$
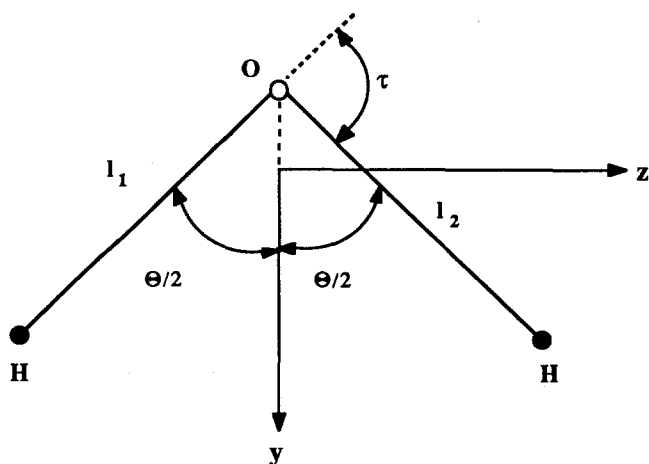

FIG. 1. The original configuration and coordinates for the water molecule which are the starting point of our calculation. The molecule is vibrationally distorted where θ is the bending angle and τ is the angle supplementary to it; l_1 and l_2 are bond lengths. The origin of the molecular axis system is at the instantaneous center-of-mass. The orientation of the molecular axes will not change during the molecular vibration.
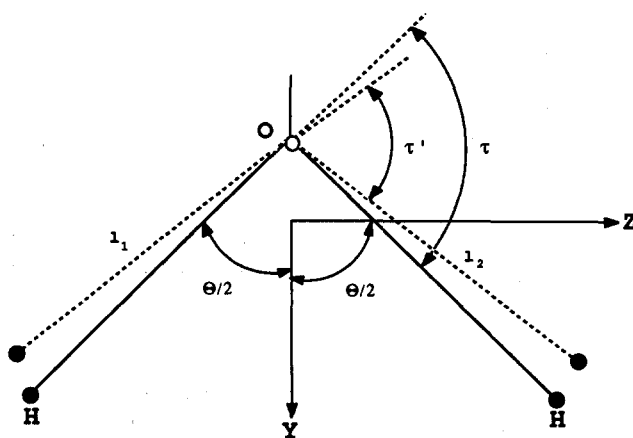

FIG. 2. The configuration and coordinates of the water molecule after the R transformation. The solid line is the distorted molecule as in Fig. 1. The R transformation yields a new LAC, τ', which depends upon both bending and stretching modes. The molecular axis system is the same as defined before the R transformation.

where

$$\eta = m/M . \tag{5}$$

In Eqs. (4) and (5) m is the atomic mass of the hydrogen atom, M is the molecular mass of H_2O, and l is the bond length in the equilibrium position. Figure 2 shows the configuration and coordinates of the H_2O molecule after the R transformation. According to Eq. (16) of I, all kinetic energy coefficients are re-expanded as a power series of S_+ and S_- under the R transformation. The S_+ dependence term of τ' goes to the higher order terms in the expansions. Then the expansion coefficients are explicit functions of $\tau' = \tau$. The vibrational stretching coordinates, S_+ and S_-, are not changed under the R transformation.

Following the R transformation, the T transformation is applied to delete the zeroth order vibration–rotation Coriolis interactions. For the H_2O molecule, the only nonzero, zeroth order vibration–rotation interaction kinetic energy coefficient is X_{x-}. From Eq. (26) of I, The only nonvanishing T-transformation coefficient is then ρ_{-}^x. As discussed in I, the T transformation is a rotation of molecular axes which depends upon the molecular vibrations. According to Eq. (27) of I, all kinetic energy coefficients are again re-expanded as a power series of S_+ and S_- through the vibrational dependence of the T transformation. The internal coordinates, S_+, S_-, and τ', are not changed. However, the zeroth order Coriolis coupling, X_{x-}'', vanishes after the T transformation.

After the R and T transformations, the zeroth order kinetic energy tensor is diagonal since there is no zeroth order rotation–LAM interaction for H_2O. The zeroth order kinetic energy coefficients in momentum space are

$$\mu_{xx}^{(0)} = \tfrac{1}{2}m^{-1}l^{-2}(1 - \eta + \eta c)^{-1} , \tag{6a}$$

$$\mu_{yy}^{(0)} = m^{-1}l^{-2}(1 + c)^{-1} , \tag{6b}$$

$$\mu_{zz}^{(0)} = m^{-1}l^{-2}(1 - c)^{-1}(1 - 2\eta)^{-1} , \tag{6c}$$

$$\mu_{\tau\tau}^{(0)} = 2m^{-1}l^{-2}(1 - \eta - \eta c)^{-1} , \tag{6d}$$

$$G_{++}^{(0)} = m^{-1}(1 - 2\eta)^{-1}(1 - \eta - \eta c) , \tag{6e}$$

$$G_{--}^{(0)} = m^{-1}(1 - 2\eta)^{-1}(1 - \eta + \eta c) , \tag{6f}$$

with

$$c = \cos(\tau') , \tag{7}$$

where m, l, and η are defined in Eqs. (4) and (5). These kinetic energy coefficients are now functions of the new LAC, τ'.

The normal coordinate transformation is especially simple since there is no interaction between the vibrational coordinates S_+ and S_-. Then the coefficients of the normal coordinate transformation are

$$L_{++} = \sqrt{G^0_{++}}, \quad L_{--} = \sqrt{G^0_{--}} , \tag{8}$$

where G^0_{++} and G^0_{--} are taken at the equilibrium position of the bending angle and are therefore τ' independent. With the independent harmonic force constant F^0_{++} and

F^0_{--}, the vibrational frequencies are

$$\omega_+ = \sqrt{G^0_{++} F^0_{++}}, \quad \omega_- = \sqrt{G^0_{--} F^0_{--}}, \tag{9}$$

and are likewise τ' independent. The bending angle dependent portion of the G- and F-matrix elements is taken account of in the perturbation terms. The normal coordinate transformation yields a vibrational basis, i.e., the two harmonic oscillator eigenfunctions with the vibrational frequencies ω_+ and ω_-. These will be used as the basis for the Van Vleck perturbation scheme.

The first and second order nonvanishing kinetic energy coefficients in the normal coordinate basis and momentum space are

$$\mu^+_{xx} = -\frac{1}{\sqrt{2}} m^{-1} l^{-3} L_{++} (1-2\eta)(1-\eta-\eta c)^{-1}(1-\eta+\eta c)^{-2} , \tag{10a}$$

$$\mu^+_{yy} = -\sqrt{2} m^{-1} l^{-3} L_{++} (1+c)^{-1}(1-2\eta)(1-\eta-\eta c)^{-1} , \tag{10b}$$

$$\mu^+_{zz} = -\sqrt{2} m^{-1} l^{-3} L_{++} (1-c)^{-1}(1-2\eta)^{-1}(1-\eta-\eta c)^{-1} , \tag{10c}$$

$$\mu^+_{\tau\tau} = -2\sqrt{2} m^{-1} l^{-3} L_{++} (1-2\eta)(1-\eta-\eta c)^{-3} , \tag{10d}$$

$$\mu^-_{yz} = -\sqrt{2} m^{-1} l^{-3} L_{--} s^{-1}(1-\eta+\eta c)^{-1} , \tag{10e}$$

$$\mu^-_{x\tau} = \sqrt{2} m^{-1} l^{-3} L_{--} (1-2\eta)(1-\eta-\eta c)^{-1}(1-\eta+\eta c)^{-2} , \tag{10f}$$

$$\mu^-_{x+} = -\tfrac{1}{2} m^{-1} l^{-2} L_{--} L^{-1}_{++} \eta s (1-2\eta)^{-1} , \tag{10g}$$

$$\mu^+_{x-} = -\tfrac{1}{2} m^{-1} l^{-2} L_{++} L^{-1}_{--} \eta s (1-2\eta)^{-1}(1-\eta+\eta c)(1-\eta-\eta c)^{-1} , \tag{10h}$$

$$\mu^+_{\tau i} = -m^{-1} l^{-2} \eta s (1-2\eta)^{-1}(1-\eta-\eta c)^{-2}(1-2\eta-\eta^2 s^2) , \tag{10i}$$

$$\mu^-_{\tau -} = m^{-1} l^{-2} \eta s (1-2\eta)^{-1}(1-\eta-\eta c)^{-1}(1-\eta+\eta c)^{-1}(1-2\eta+4\eta^2+4\eta c-4\eta^2 c) , \tag{10j}$$

$$\mu^{++}_{xx} = m^{-2} l^{-4} (1-2\eta)^{-1}(1-\eta-\eta c_0)(1-\eta-\eta c)^{-2}(1-\eta+\eta c)^{-1} \big[(1-2\eta)^2(1-\eta+\eta c)^{-2}$$
$$\qquad -\tfrac{1}{4}(1-\eta-\eta c)^2 + \tfrac{1}{4}\eta^2 s^2 (1-2\eta)^{-1}(1-\eta+\eta c)^2$$
$$\qquad + \tfrac{1}{2}\eta^2 s^2 (1-\eta-\eta c)^{-1}(2-4\eta-\eta c+\eta^2 c+\eta^2 c^2) \big] , \tag{10k}$$

$$\mu^{--}_{xx} = m^{-2} l^{-4} (1-\eta+\eta c_0)\big[(1-2\eta)(1-\eta-\eta c)^{-1}(1-\eta+\eta c)^{-4} -\tfrac{1}{4}(1-2\eta)^{-1}(1-\eta-\eta c)$$
$$\qquad \times (1-\eta+\eta c)^{-2} + \tfrac{1}{4}\eta^2 s^2 (1-2\eta)^{-2}(1-\eta-\eta c)^{-1} \big] , \tag{10l}$$

$$\mu^{++}_{yy} = 2m^{-2} l^{-4} (1+c)^{-1}(1-\eta-\eta c_0)(1-2\eta)^{-1}\big[(1-2\eta)^2(1-\eta-\eta c)^{-2} -\tfrac{1}{4}+\tfrac{1}{2}\eta(1-c)$$
$$\qquad \times (1-\eta-\eta c)^{-3}(2-4\eta-\eta c+\eta^2 c+\eta^2 c^2) \big] , \tag{10m}$$

$$\mu^{--}_{yy} = 2m^{-2} l^{-4} (1+c)^{-1}(1-\eta+\eta c_0)(1-\eta+\eta c)^{-2}\big[1-\tfrac{1}{4}(1-2\eta)^{-1}(1-2\eta c-3\eta^2+4\eta^2 c-\eta^2 c^2) \big] , \tag{10n}$$

$$\mu^{++}_{zz} = 2m^{-2} l^{-4} (1-c)^{-1}(1-\eta-\eta c_0)(1-2\eta)^{-2}\big[(1-\eta-\eta c)^{-2} -\tfrac{1}{4}-\tfrac{1}{2}\eta(1+c)$$
$$\qquad \times (1-\eta-\eta c)^{-3}(2-4\eta-\eta c+\eta^2 c+\eta^2 c^2) \big] , \tag{10o}$$

$$\mu^{--}_{zz} = 2m^{-2} l^{-4} (1-c)^{-1}(1-\eta+\eta c_0)(1-2\eta)^{-2}(1-\eta+\eta c)^{-2}(\tfrac{3}{4}-\eta+\tfrac{1}{2}\eta c-\tfrac{1}{4}\eta^2+\tfrac{1}{4}\eta^2 c^2) , \tag{10p}$$

$$\mu^{++}_{\tau\tau} = 4m^{-2} l^{-4} (1-2\eta)^{-1}(1-\eta-\eta c_0)(1-\eta-\eta c)^{-5}\big[1-4\eta-2\eta c+4\eta^2-\tfrac{1}{4}(1-\eta-\eta c)^4$$
$$\qquad + \tfrac{1}{4}\eta^2 s^2 (1-2\eta)^{-1}(1-2\eta-\eta^2 s^2)^2 + 3\eta^2(1+2c) - \tfrac{5}{2}\eta^3(1+c)(2-c+c^2)$$
$$\qquad - \tfrac{1}{2}\eta^4(1+2c+c^2)(4+c+c^2) \big] , \tag{10q}$$

$$\mu^{--}_{\tau\tau} = 4m^{-2} l^{-4} (1-2\eta)^{-1}(1-\eta+\eta c_0)(1-\eta+\eta c)^{-3}(1-\eta-\eta c)^{-2}\big[(1-\eta)^2 -\tfrac{1}{4}(1-\eta+\eta c)^4$$
$$\qquad + \eta(c+\eta-\eta c)(2-4\eta+\eta c+2\eta^2-\eta^2 c-\eta^2 c^2)$$
$$\qquad + \tfrac{1}{4}\eta^2 s^2 (1-2\eta)^{-1}(1-6\eta+4\eta c+4\eta^2-4\eta^2 c)^2 \big] . \tag{10r}$$

$$g_{++} = \eta(c_0-c)(1-\eta-\eta c_0)^{-1} , \tag{11a}$$

$$g_{--} = -\eta(c_0 - c)(1 - \eta + \eta c_0)^{-1}, \tag{11b}$$

where

$$s = \sin(\tau'), \quad c_0 = \cos(\tau_0), \text{ etc.;} \tag{12}$$

τ_0 is the supplementary bending angle at the equilibrium position, with $\tau_0 + \theta_0 = \pi$. c and η are defined by Eqs. (5) and (7); and g_{++} and g_{--} are the bending angle dependent parts of the G-matrix elements after the normal coordinate transformation.

The potential energy coefficients also depend explicitly upon the LAC, τ, just as the kinetic energy coefficients do. These potential energy coefficients are modified by the R transformation. Except for the pure stretching vibrational terms which are included in Eq. (9), the τ' dependent potential energy in the normal coordinate basis is

$$
\begin{aligned}
V = V(\tau') &+ f_+(\tau')Q_+ + (1/2)f_{++}(\tau')Q_+^2 + (1/2)f_{--}(\tau')Q_-^2 \\
&+ (1/6)f_{+++}(\tau')Q_+^3 + (1/2)f_{+--}(\tau')Q_+Q_-^2 + (1/24)f_{++++}(\tau')Q_+^4 \\
&+ (1/24)f_{----}(\tau')Q_-^4 + (1/4)f_{++--}(\tau')Q_+^2 Q_-^2 ,
\end{aligned} \tag{13}
$$

where

$$V(\tau') = \tfrac{1}{2}F_{\tau\tau}(\tau' - \tau_0)^2 + \tfrac{1}{6}F_{\tau\tau\tau}(\tau' - \tau_0)^3 + \tfrac{1}{24}F_{\tau\tau\tau\tau}(\tau' - \tau_0)^4 , \tag{14a}$$

$$f_+ = L_{++}\{F_{+\tau}(\tau' - \tau_0) + \tfrac{1}{2}F_{\tau\tau+}(\tau' - \tau_0)^2 - R_{\tau+}[F_{\tau\tau}(\tau' - \tau_0) + \tfrac{1}{2}F_{\tau\tau\tau}(\tau' - \tau_0)^2 + \tfrac{1}{6}F_{\tau\tau\tau\tau}(\tau' - \tau_0)^3]\}, \tag{14b}$$

$$
\begin{aligned}
f_{++} = (L_{++})^2\{&F_{++\tau}(\tau' - \tau_0) + \tfrac{1}{2}F_{++\tau\tau}(\tau' - \tau_0)^2 - 2R_{\tau+}[F_{+\tau} + F_{+\tau\tau}(\tau' - \tau_0)] + 2R_{\tau+}\frac{\partial R_{\tau+}}{\partial \tau} \\
&\times [F_{\tau\tau}(\tau' - \tau_0) + \tfrac{1}{2}F_{\tau\tau\tau}(\tau' - \tau_0)^2 + \tfrac{1}{6}F_{\tau\tau\tau\tau}(\tau' - \tau_0)^3]\},
\end{aligned} \tag{14c}
$$

$$f_{--} = (L_{--})^2\{F_{--\tau}(\tau' - \tau_0) + \tfrac{1}{2}F_{--\tau\tau}(\tau' - \tau_0)^2\}, \tag{14d}$$

$$f_{+--} = L_{++}(L_{--})^2\{F_{+--} - R_{\tau+}[F_{--\tau} + F_{--\tau\tau}(\tau - \tau_0)]\}, \tag{14e}$$

$$
\begin{aligned}
f_{+++} = (L_{++})^3\{&F_{+++} - (R_{\tau+})^3[F_{\tau\tau\tau} + F_{\tau\tau\tau\tau}(\tau' - \tau_0)] - 3R_{\tau+}[F_{++\tau} + F_{++\tau\tau}(\tau' - \tau_0)] \\
&+ 3(R_{\tau+})^2 F_{\tau\tau+} - 3(R_{\tau+})^2 \frac{\partial^2 R_{\tau+}}{\partial \tau^2}[F_{\tau\tau}(\tau' - \tau_0) + \tfrac{1}{2}F_{\tau\tau\tau}(\tau' - \tau_0)^2 \\
&+ \tfrac{1}{6}F_{\tau\tau\tau\tau}(\tau' - \tau_0)^3] - 6R_{\tau+}\left(\frac{\partial R_{\tau+}}{\partial \tau}\right)^2[F_{\tau\tau}(\tau' - \tau_0) + \tfrac{1}{2}F_{\tau\tau\tau}(\tau' - \tau_0)^2 + \tfrac{1}{6}F_{\tau\tau\tau\tau}(\tau' - \tau_0)^3] \\
&+ 6R_{\tau+}\frac{\partial R_{\tau+}}{\partial \tau}[F_{+\tau} + F_{+\tau\tau}(\tau' - \tau_0)] - 6(R_{\tau+})^2\frac{\partial R_{\tau+}}{\partial \tau}[F_{\tau\tau} + F_{\tau\tau\tau}(\tau' - \tau_0) + \tfrac{1}{2}F_{\tau\tau\tau\tau}(\tau' - \tau_0)^2]\},
\end{aligned} \tag{14f}
$$

$$
\begin{aligned}
f_{++++} = (L_{++})^4\{&F_{++++} + F_{\tau\tau\tau\tau}(R_{\tau+})^4 + 6F_{++\tau\tau}(R_{\tau+})^2 + 12(R_{\tau+})^3\frac{\partial R_{\tau+}}{\partial \tau}[F_{\tau\tau\tau} + F_{\tau\tau\tau\tau}(\tau' - \tau_0)] \\
&- 24F_{+\tau\tau}(R_{\tau+})^2\frac{\partial R_{\tau+}}{\partial \tau} + 12R_{\tau+}\frac{\partial R_{\tau+}}{\partial \tau}[F_{++\tau} + F_{++\tau\tau}(\tau' - \tau_0)] + 36(R_{\tau+})^2\left(\frac{\partial R_{\tau+}}{\partial \tau}\right)^2 \\
&\times [F_{\tau\tau} + F_{\tau\tau\tau}(\tau' - \tau_0) + \tfrac{1}{2}F_{\tau\tau\tau\tau}(\tau' - \tau_0)^2] + 12(R_{\tau+})^3\frac{\partial^2 R_{\tau+}}{\partial \tau^2}[F_{\tau\tau} + F_{\tau\tau\tau}(\tau' - \tau_0) \\
&+ \tfrac{1}{2}F_{\tau\tau\tau\tau}(\tau' - \tau_0)^2] - 12(R_{\tau+})^2\frac{\partial^2 R_{\tau+}}{\partial \tau^2}[F_{+\tau} + F_{+\tau\tau}(\tau' - \tau_0)] - 24R_{\tau+}\left(\frac{\partial R_{\tau+}}{\partial \tau}\right)^2 \\
&\times [F_{+\tau} + F_{+\tau\tau}(\tau' - \tau_0)] + 4(R_{\tau+})^3\frac{\partial^3 R_{\tau+}}{\partial \tau^3}[F_{\tau\tau}(\tau' - \tau_0) + \tfrac{1}{2}F_{\tau\tau\tau}(\tau' - \tau_0)^2 + \tfrac{1}{6}F_{\tau\tau\tau\tau}(\tau' - \tau_0)^3] \\
&+ 36(R_{\tau+})^2\frac{\partial R_{\tau+}}{\partial \tau}\frac{\partial^2 R_{\tau+}}{\partial \tau^2}[F_{\tau\tau}(\tau' - \tau_0) + \tfrac{1}{2}F_{\tau\tau\tau}(\tau' - \tau_0)^2 + \tfrac{1}{6}F_{\tau\tau\tau\tau}(\tau' - \tau_0)^3] + 24R_{\tau+}\left(\frac{\partial R_{\tau+}}{\partial \tau}\right)^3 \\
&\times [F_{\tau\tau}(\tau' - \tau_0) + \tfrac{1}{2}F_{\tau\tau\tau}(\tau' - \tau_0)^2 + \tfrac{1}{6}F_{\tau\tau\tau\tau}(\tau' - \tau_0)^3]\},
\end{aligned} \tag{14g}
$$

$$f_{----} = (L_{--})^4 F_{----}, \tag{14h}$$

$$f_{--++} = (L_{++})^2(L_{--})^2\{F_{--++} + F_{--\tau\tau}(R_{\tau+})^2 + 2R_{\tau+}\frac{\partial R_{\tau+}}{\partial \tau}[F_{--\tau} + F_{--\tau\tau}(\tau' - \tau_0)]\}. \tag{14i}$$

$R_{\tau+}$ is defined in Eq. (4) and the force constants $F_{\tau\tau}, F_{\tau+}, F_{+++}$, etc., are determined either experimentally or by *ab initio* calculations.

The anharmonic vibrational coefficients in Eq. (2), when expanded in terms of the kinetic and potential energy coeffi-

cients, become

$$\chi_{++} = \tfrac{3}{2}f_{++++}\omega_+^{-2} - \tfrac{15}{4}(f_{+++})^2\omega_+^{-4}, \tag{15a}$$

$$\chi_{--} = \tfrac{3}{2}f_{----}\omega_-^{-2} - \tfrac{1}{4}(f_{--+})^2(\omega_+\omega_-)^{-2}(8\omega_-^2 - 3\omega_+^2)(4\omega_-^2 - \omega_+^2)^{-1}, \tag{15b}$$

$$\chi_{+-} + \chi_{-+} = f_{++--}(\omega_+\omega_-)^{-1} - 3f_{+++}f_{---}\omega_+^{-3}\omega_-^{-1} - 2(f_{--+})^2(\omega_+\omega_-)^{-1}(4\omega_-^2 - \omega_+^2)^{-1}. \tag{15c}$$

These coefficients are especially simple since no G-matrix elements for the stretching modes contribute directly.

Now the effective rotation–LAM Hamiltonian, $H_{\tau R}^{\text{eff}}$, can be rearranged as follows:

$$H_{\tau R}^{\text{eff}} = H_\tau^{\text{eff}} + H_R^{\text{eff}}, \tag{16}$$

where

$$\begin{aligned}
H_\tau^{\text{eff}} &= H_\tau^0 + H_\tau' + H_{\tau,+}'(n_+ + 1/2) + H_{\tau,-}'(n_- + 1/2) + \chi_{++}(n_+ + 1/2)^2 + \chi_{--}(n_- + 1/2)^2 \\
&\quad + (\chi_{+-} + \chi_{-+})(n_+ + 1/2)(n_- + 1/2) \\
&= (1/2)\mu_{\tau\tau}^{\text{eff}}P_\tau^2 + (1/4)\mu_{\tau\tau\tau\tau}P_\tau^4 + V_{\text{eff}},
\end{aligned} \tag{17a}$$

$$\begin{aligned}
H &= H_R^0 + H_R' + H_{R,+}'(n_+ + 1/2) + H_{R,-}'(n_- + 1/2) \\
&\quad + H_{\tau R}^0 + H_{\tau R}' + H_{\tau R,+}'(n_+ + 1/2) + H_{\tau R,-}'(n_- + 1/2) + H_{\text{CD}} \\
&= (1/2)\mu_{xx}^{\text{eff}}P_x^2 + (1/2)\mu_{yy}^{\text{eff}}P_y^2 + (1/2)\mu_{zz}^{\text{eff}}P_z^2 + H_{\text{CD}}.
\end{aligned} \tag{17b}$$

The terms of Eqs. (17(a) and 17(b)) are expressed as

$$\begin{aligned}
\mu_{\tau\tau}^{\text{eff}} &= \mu_{\tau\tau}^{(0)} - \omega_+^{-2}f_+\mu_{\tau\tau}^+ - \omega_+^{-4}(\mu_{\tau\tau}^{(0)})^2\left(\frac{\partial f_+}{\partial\tau}\right)^2 + (n_+ + \tfrac{1}{2})\Big[\omega_+^{-1}\mu_{\tau\tau}^{++} + \tfrac{1}{2}\omega_+^{-1}g_{++}\mu_{\tau\tau}^{++} - \tfrac{1}{2}\omega_+^{-3}f_{++}\mu_{\tau\tau}^{++} \\
&\quad \times - \tfrac{1}{2}\omega_+^{-3}f_{+++}\mu_{\tau\tau}^+ - \omega_+^{-1}(\mu_{\tau+}^+)^2 + \omega_+^{-3}\mu_{\tau\tau}^{(0)}\frac{\partial f_+}{\partial\tau}\Big] + (n_- + \tfrac{1}{2})\Big[\omega_-^{-1}\mu_{\tau\tau}^{--} \\
&\quad + \tfrac{1}{2}\omega_-^{-1}g_{--}\mu_{\tau\tau}^{--} - \tfrac{1}{2}\omega_-^{-3}f_{--}\mu_{\tau\tau}^{--} - \omega_-^{-1}(\mu_{\tau-}^-)^2 - \tfrac{1}{2}\omega_1^{-1}\omega_+^{-2}f_{--+}\mu_{\tau\tau}^+\Big],
\end{aligned} \tag{18}$$

$$\mu_{\tau\tau\tau\tau}^{\text{eff}} = -\tfrac{1}{2}\omega_+^{-2}(\mu_{\tau\tau}^+)^2 - \tfrac{1}{2}\omega_+^{-3}(\mu_{\tau\tau}^{++})^2(n_+ + \tfrac{1}{2}) - \tfrac{1}{2}\omega_-^{-3}(\mu_{\tau\tau}^{--})^2(n_- + \tfrac{1}{2}), \tag{19}$$

$$\begin{aligned}
V_{\text{eff}} &= V(\tau) - \tfrac{1}{2}\omega_+^{-2}(f_+)^2 + \tfrac{1}{2}\omega_+^{-4}(f_+)^2f_{++} + (n_+ + \tfrac{1}{2})\Big[\tfrac{1}{2}\omega_+^{-1}f_{++} + \tfrac{1}{2}\omega_+g_{++} \\
&\quad - \tfrac{1}{2}\omega_+^{-3}f_+f_{+++} - \tfrac{1}{8}\omega_+(g_{++})^2 - \tfrac{1}{8}\omega_+^{-3}(f_{++})^2 + \tfrac{1}{4}\omega_+^{-1}f_{++}g_{++}\Big] \\
&\quad + (n_- + \tfrac{1}{2})\Big[\tfrac{1}{2}\omega_-^{-1}f_{--} + \tfrac{1}{2}\omega_-g_{--} - \tfrac{1}{8}\omega_-(g_{--})^2 - \tfrac{1}{8}\omega_-^{-3}f_{--}^2 + \tfrac{1}{4}\omega_-^{-1}f_{--}g_{--} - \tfrac{1}{4}\omega_-^{-1}\omega_+^{-2}f_+f_{--+}\Big] \\
&\quad + \chi_{++}(n_+ + \tfrac{1}{2})^2 + (\chi_{+-} + \chi_{-+})(n_+ + \tfrac{1}{2})(n_- + \tfrac{1}{2}) + \chi_{--}(n_- + \tfrac{1}{2})^2,
\end{aligned} \tag{20}$$

$$\begin{aligned}
\mu_{xx}^{\text{eff}} &= \mu_{xx}^{(0)} - \omega_+^{-2}f_+\mu_{xx}^+ - \tfrac{1}{2}\omega_+^{-2}\mu_{xx}^+(\mu_{\tau\tau}^+P_\tau^2) - \omega_-^{-2}(\mu_{x\tau}^-P_\tau)^2 + (n_+ + \tfrac{1}{2})\{\omega_+^{-1}\mu_{xx}^{++} \\
&\quad - \tfrac{1}{2}\omega_+^{-3}\mu_{xx}^+f_{+++} + \tfrac{1}{2}\omega_+^{-1}g_{++}\mu_{xx}^{++} - \tfrac{1}{2}\omega_+^{-3}f_{++}\mu_{xx}^{++} + \omega_+^{-1}(\omega_+^2 - \omega_-^2)^{-1} \\
&\quad \times [\omega_+^2(\mu_{x+}^-)^2 + \omega_-^2(\mu_{x-}^-)^2 - 2\omega_+^2\mu_{x+}^-\mu_{x-}^-] - \tfrac{1}{2}\omega_+^{-3}\mu_{xx}^{++}\mu_{\tau\tau}^{++}P_\tau^2\} \\
&\quad + (n_- + \tfrac{1}{2})\{\omega_-^{-1}\mu_{xx}^{--} + \tfrac{1}{2}\omega_-^{-1}g_{--}\mu_{xx}^{--} - \tfrac{1}{2}\omega_-^{-3}f_{--}\mu_{xx}^{--} - \tfrac{1}{2}\omega_-^{-1}\omega_+^{-2}\mu_{xx}^+f_{--+} \\
&\quad - \omega_-^{-1}(\omega_+^2 - \omega_-^2)^{-1}[\omega_-^2(\mu_{x-}^+)^2 + \omega_+^2(\mu_{x+}^-)^2 - 2\omega_-^2\mu_{x+}^-\mu_{x-}^+] - \tfrac{1}{2}\omega_-^{-3}\mu_{xx}^{--}\mu_{\tau\tau}^{--}P_\tau^2\},
\end{aligned} \tag{21a}$$

$$\begin{aligned}
\mu_{yy}^{\text{eff}} &= \mu_{yy}^{(0)} - \omega_+^{-2}f_+\mu_{yy}^+ - \tfrac{1}{2}\omega_+^{-2}\mu_{yy}^+\mu_{\tau\tau}^+P_\tau^2 + (n_+ + \tfrac{1}{2})\Big[\omega_+^{-1}\mu_{yy}^{++} - \tfrac{1}{2}\omega_+^{-3}\mu_{yy}^+f_{+++} \\
&\quad + \tfrac{1}{2}\omega_+^{-1}\mu_{yy}^{++}g_{++} - \tfrac{1}{2}\omega_+^{-3}f_{++}\mu_{yy}^{++} - \frac{\omega_+^{-3}}{2}\mu_{yy}^{++}\mu_{\tau\tau}^{++}P_\tau^2\Big] + (n_- + \tfrac{1}{2})\Big[\omega_-^{-1}\mu_{yy}^{--} \\
&\quad + \tfrac{1}{2}\omega_-^{-1}g_{--}\mu_{yy}^{--} - \tfrac{1}{2}\omega_-^{-3}f_{--}\mu_{yy}^{--} - \tfrac{1}{2}\omega_-\omega_+^{-2}f_{--+}\mu_{yy}^+ - \tfrac{1}{2}\omega_-^{-3}\mu_{yy}^{--}\mu_{\tau\tau}^{--}P_\tau^2\Big],
\end{aligned} \tag{21b}$$

$$\begin{aligned}
\mu_{zz}^{\text{eff}} &= \mu_{zz}^{(0)} - \omega_+^{-2}f_+\mu_{zz}^+ - \tfrac{1}{2}\omega_+^{-2}\mu_{zz}^+\mu_{\tau\tau}^+P_\tau^2 + (n_+ + \tfrac{1}{2})\Big[\omega_+^{-1}\mu_{zz}^{++} - \tfrac{1}{2}\omega_+^{-3}\mu_{zz}^+f_{+++} \\
&\quad + \tfrac{1}{2}\omega_+^{-1}g_{++}\mu_{zz}^{++} - \tfrac{1}{2}\omega_+^{-3}f_{++}\mu_{zz}^{++} - \tfrac{1}{2}\omega_+^{-3}\mu_{zz}^{++}\mu_{\tau\tau}^{++}P_\tau^2\Big] + (n_- + \tfrac{1}{2})\Big[\omega_-^{-1}\mu_{zz}^{--} \\
&\quad + \tfrac{1}{2}\omega_-^{-1}g_{--}\mu_{zz}^{--} - \tfrac{1}{2}\omega_-^{-3}f_{--}\mu_{zz}^{--} - \tfrac{1}{2}\omega_-^{-1}\omega_+^{-2}f_{--+}\mu_{zz}^+ - \tfrac{1}{2}\omega_-^{-3}\mu_{zz}^{--}\mu_{\tau\tau}^{--}P_\tau^2\Big],
\end{aligned} \tag{21c}$$

$$\begin{aligned}
H_{\text{CD}} &= \tfrac{1}{8}\omega_+^{-2}\big[(\mu_{xx}^+)^2P_x^4 + (\mu_{yy}^+)^2P_y^4 + (\mu_{zz}^+)^2P_z^4 + \mu_{xx}^+\mu_{yy}^+(P_x^2P_y^2 + P_y^2P_x^2) + \mu_{xx}^+\mu_{zz}^+ \\
&\quad \times (P_x^2P_z^2 + P_z^2P_x^2) + \mu_{yy}^+\mu_{zz}^+(P_y^2P_z^2 + P_z^2P_y^2)\big] - \tfrac{1}{8}\omega_-^{-2}(\mu_{yz}^-)^2(P_yP_zP_yP_z \\
&\quad + P_yP_zP_zP_y + P_zP_yP_yP_z + P_zP_yP_zP_y) - \tfrac{1}{2}\omega_-^{-2}\mu_{yz}^-\mu_{x\tau}^-P_\tau(P_xP_yP_z + P_yP_zP_x).
\end{aligned} \tag{22}$$

Each coefficient of Eqs. (18)–(22) is explicitly τ' dependent. Coefficients related to P_τ, i.e., the conjugate momentum of

τ', need to be properly Hermitianized as shown in Eqs. (71)–(76) of I. The anharmonic vibrational energy operator $\Sigma \chi_{kk'}(n_k + 1/2)(n_{k'} + 1/2)$ is added into $H_{\tau R}^{\text{eff}}$ because of the τ' dependence in the $\chi_{kk'}$. The pure bending energy levels are calculated by setting n_+ and n_- equal to zero, this is referred to as the "ground vibrational state."

III. THE BASIS FUNCTIONS FOR THE LAM AND ROTATIONAL MOTION

The calculation of the vibration–rotation–LAM energy levels for the H_2O molecule can be divided into two stages. First, there is the numerical integration stage where a suitable basis is chosen for the LAM and rotation. The matrix elements of the effective rotation–LAM Hamiltonian are calculated in this basis. Second, there is the matrix diagonalization stage, where the matrices calculated from the first stage are diagonalized to obtain the rotational eigenenergies for the different vibration–LAM states.

For convention of the calculation, the effective LAM–rotation Hamiltonian can be written as

$$H_{\tau R}^{\text{eff}} = H_{\tau R}^{\text{eff}}(1) + H_{\tau R}^{\text{eff}}(2) , \qquad (23)$$

where

$$H_{\tau R}^{\text{eff}}(1) = H_{\tau}^{\text{eff}} + (1/2)\mu_{zz}^{\text{eff}} P_z^2 \qquad (24a)$$

and

$$H_{\tau R}^{\text{eff}}(2) = (1/2)\mu_{xx}^{\text{eff}} P_x^2 + (1/2)\mu_{yy}^{\text{eff}} P_y^2 + H_{\text{CD}} . \qquad (24b)$$

For the zero angular momentum state, Eq. (24a) gives the "pure" LAM Hamiltonian when the ground state is taken for the stretching vibrations. For the nonzero angular momentum states, the Schrödinger equation for $H_{\tau R}^{\text{eff}}(1)$ is solved to obtain a basis. Then the total effective rotation–LAM Hamiltonian is diagonalized in this basis to obtain the rotational energy levels for different vibration–LAM states.

The first step of our calculation has been to solve

$$H_{\tau R}^{\text{eff}}(1)\psi_n = E_n(1)\psi_n , \qquad (25)$$

where $E_n(1)$ are the intermediate diagonal values for $H_{\tau R}^{\text{eff}}(1)$ and ψ_n are used as basis functions for the total LAM-rotation Hamiltonian. The ψ_n depend upon the LAC and the three Euler angles which give the orientation for the overall rotation. The subscript n for $E_n(1)$ and ψ_n denote four quantum numbers: n_τ is quantum number of the bending motion, J is the quantum number of the total angular momentum, K is the quantum number of the component of the total angular momentum along the molecule fixed z axis, and M is the quantum number of the component of the total angular momentum along the space fixed Z axis. In the following discussion the quantum number M is omitted because of degeneracy in the absence of an external field. By separating variables, the trial basis function $\psi_{n_\tau JK}$ can be written as

$$\psi_{n_\tau JK} = \phi_{n_\tau K} S_{JK} , \qquad (26)$$

where the $\phi_{n_\tau K}$ are functions of τ' and the S_{JK} are the usual Wang functions for the rotational basis which are eigenfunctions of a symmetric rigid rotor with the three Euler angles as variables. Substitution of Eq. (26) into Eq. (25), with $P_z^2 S_{JK} = K^2 S_{JK}$, simplifies Eq. (25) to

$$(H_{\tau}^{\text{eff}} + 1/2K^2\mu_{zz}^{\text{eff}})\phi_{n_\tau K} = E_{n_\tau K}(1)\phi_{n_\tau K} . \qquad (27)$$

Therefore $\phi_{n_\tau K}$ is an eigenfunction of the operator

$H_{\tau}^{\text{eff}} + (1/2)K^2\mu_{zz}^{\text{eff}}$. The pure bending energy levels can be calculated by setting $J = 0$ and $K = 0$ in Eq. (27). To summarize, $\psi_{n_\tau JK}$ are eigenfunctions of $H_{\tau R}^{\text{eff}}(1)$ and basis functions for the calculation of the rotational energy levels for the different vibration–LAM states. $E_{n_\tau K}(1)$ are intermediate results but not an "actual" energy eigenvalue except for the zero angular momentum states. The above treatment parallels that of the HBJ theory.[4]

The total effective LAM–rotation Hamiltonian is invariant under inversion of the LAC, τ', i.e., $H(\tau') = H(-\tau')$. This requires that the basis functions $\phi_{n_\tau K}$ have a definite parity with respect to τ'. Figure 3 shows the shape of the basis functions $\phi_{n_\tau K}$ with even and odd parities. Since both the HMS[1] and HB[4(d)] constants which are used in the present approach are high barrier approximations (the barrier height is 13 182.9 cm^{-1} for the HMS constants and is 12 512.9 cm^{-1} for the HB constants), the energy $E_{n_\tau K}(1)$ in Eq. (27) is parity degenerate for low n_τ and K, $n_\tau \leqslant 3$ and $K \leqslant 10$. On the other hand, the total LAM–rotation effective Hamiltonian has a period 2π for τ'. This requires that the basis functions have period 2π. Since singular points exist in the numerical integration at the points shown in Eqs. (29a)–(29d), the basis functions with odd parity are used for the rotational energy calculation. The basis function with odd parity can be expanded as Fourier sine series

$$\phi_{n_\tau K} = \sum_i A_{n_\tau K}^i \sin(i\tau') , \quad i = 1,2,3,..., \qquad (28)$$

where $A_{n_\tau K}^i$ is the expansion coefficient. Equation (27) is solved by numerical integration in the basis of the Fourier sine functions to obtain $E_{n_\tau K}(1)$ and $\phi_{n_\tau K}$. Then matrix elements of $H_{\tau R}^{\text{eff}}(2)$ are integrated in the $\psi_{n_\tau JK}$ basis. Finally, diagonalization of the matrix of the total effective Hamiltonian yields the desired rotational eigenenergies for the different LAM–vibration states.

The singular points for the various terms of the total effective LAM–rotation Hamiltonian come from

$$\mu_{zz}^{\text{eff}}|_{\tau'\to 0} \propto (1 - \cos \tau')^{-1} , \qquad (29a)$$

$$\mu_{yy}^{\text{eff}}|_{\tau'\to \pi} \propto (1 + \cos \tau')^{-1} , \qquad (29b)$$

$$H_{\text{CD}}|_{\tau'\to 0} \propto (1 - \cos \tau')^{-1}$$
$$+ A \sin^{-2} \tau' + B(1 - \cos \tau')^{-2} , \qquad (29c)$$

$$H_{\text{CD}}|_{\tau'\to \pi} \propto (1 + \cos \tau')^{-1}$$
$$+ C \sin^{-2} \tau' + D(1 + \cos \tau')^{-2} , \qquad (29d)$$

where A, B, C, and D are constants. By using the Fourier sine functions as the integration basis, except for the terms with a factor $(1 - \cos \tau')^{-2}$ or $(1 + \cos \tau')^{-2}$ in H_{CD}, the numerical integration of the terms given by Eqs. (29a)–(29d) have finite limits at the singular points. For the terms with the factors $(1 - \cos \tau')^{-2}$ or $(1 + \cos \tau')^{-2}$, the coefficients are very small. These last two terms are included in $H_{\tau R}^{\text{eff}}(2)$ and integrated in the $\psi_{n_\tau JK}$ basis which vanishes at the singu-
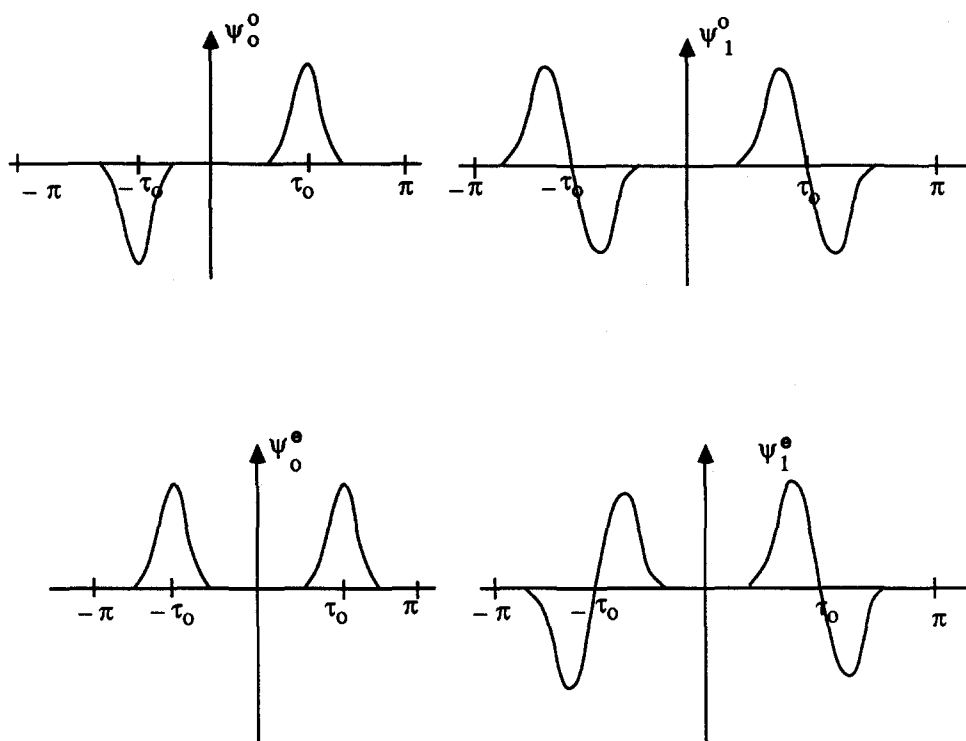
FIG. 3. The shape of the basis functions ψ_{n_τ}. ψ_0 and ψ_1, the ground state and the first-excited state of the LAM, respectively, are used as examples. The superscripts "odd" or "even" denote the odd or even parity with respect to the LAC, τ'. $\psi_{n_\tau}^o = \psi_{n_\tau}^e$ for the $0 < \tau' < \pi$ region and $\psi_{n_\tau}^o = -\psi_{n_\tau}^e$ for the $-\pi < \tau' < 0$ region. The basis functions with the same quantum numbers but the different parities give the same energy $E_{n_\tau K}$ and probability $|\phi_{n_\tau K}|^2$ to the order 10^{-3} cm^{-1} in energy and 10^{-8} in $|\phi_{n_\tau K}|^2$ up to $n_\tau = 3$. Note: φ is used for the symbol ψ_n^e and ψ_n^o in the text.

lar points. Avoiding the singular points with the Fourier sine basis in the numerical integration does not change the final results. We have confirmed this directly by the computer calculations.

Another advantage of using the Fourier sine (or cosine) series for the basis is the simplification of the Hermitian formulas for the terms related to P_τ, the conjugate momentum of τ', in the numerical integration. As a quantum mechanical operator, $P_\tau = -i(\partial/\partial\tau')$. The term $\mu_{\tau\tau}P_\tau^2$ may be considered as an example. The correct Hermitian formula is given by Eq. (71) of I where the operator form of the P related terms can be written as

$$\mu_{\tau\tau}P_\tau^2 + (P_\tau\mu_{\tau\tau})P_\tau = P_\tau\mu_{\tau\tau}P_\tau . \tag{30}$$

P_τ and $\mu_{\tau\tau}$ do not commute because of the τ' dependence of $\mu_{\tau\tau}$. The derivative of $\mu_{\tau\tau}$ yields a tedious term because $\mu_{\tau\tau}$ is a complicated function of τ'. In the Fourier sine (or cosine) basis, the numerical integral form for the matrix element of the operator $P_\tau\mu_{\tau\tau}P_\tau$ in Eq. (30) can be written as

$$(P_\tau\mu_{\tau\tau}P_\tau)_{ij} = -\int_{-\pi}^{\pi} \{\sin(i\tau')\frac{\partial}{\partial\tau'}\mu_{\tau\tau}\frac{\partial}{\partial\tau'}\sin(j\tau')\}d\tau'$$

$$= ij\int_{-\pi}^{\pi} \mu_{\tau\tau}\cos(i\tau')\cos(j\tau')d\tau' , \tag{31}$$

where i and j are integers. The last line of Eq. (31) comes from partial integration. The second term on the left side of Eq. (30), the derivative of $\mu_{\tau\tau}$, vanishes by the partial integration and the Hermitian term is included into the integral in a natural way. The numerical integration itself is also simplified since no $\partial\mu_{\tau\tau}/\partial\tau'$ terms appear in it.

IV. THE VIBRATIONAL AND LAM ENERGY LEVELS

Initially two sets of force constants and molecular geometry were used in our calculation. The first set was de-

rived by the Hoy, Mills, and Strey (HMS) analysis[1] for H_2O where bending and stretching modes were expanded as a Taylor series through quartic terms. The force constants and molecular geometry were calculated by perturbation theory to fit the observed spectra. The second set was derived by Hoy and Bunker (HB).[4(d)] Using the HBJ theory,[3] HB made modifications in some of the force constants and molecular geometry as previously determined by HMS to improve the fit with the rotational spectra up to $J = 10$ for the ground and the first excited bending states.

The vibration–LAM energy levels are calculated for the zero angular momentum state for the total effective rotation–LAM Hamiltonian, $H_{\tau R}^{\text{eff}}$, given by Eq. (16). Therefore the effective rotational Hamiltonian, H_R^{eff}, is set equal to zero and the effective LAM Hamiltonian, H_τ^{eff}, is left for the calculation. H_τ^{eff} can be divided into two parts: One part is independent of the stretching vibrational states which are denoted by the vibrational quantum numbers n_+ and n_-. The remaining part depends upon the stretching vibrational states. With the harmonic stretching frequencies ω_+ and ω_- given by Eq. (9), any special vibration–LAM energy level can be calculated by specifying the definite n_+ and n_-. Setting $n_+ = 0$ and $n_- = 0$ yields the pure LAM states.

With the specified stretching vibrational quantum numbers n_+ and n_-, the effective LAM Hamiltonian, $H_{\tau R}^{\text{eff}}$, is integrated numerically in the basis of Fourier sine functions by a computer program. The error of the numerical integration is less than 10^{-7} cm^{-1}. Diagonalization of the integrated matrix by the same computer program yields the vibration–LAM eigenenergies and LAM wave functions. The wave functions converge rapidly as series expansions of the Fourier sine functions for the lower energy states up to $n_\tau \leq 6$, where n_τ denotes the LAM states.

We found that calculations of the vibrational energies

TABLE I. This table contains the revised force constants, GQ, that were used in the present calculation. The force constants that were not changed were taken from Hoy–Mills–Strey[a] and Hoy–Bunker.[b] The equilibrium molecular structure is from Hoy–Bunker.

Force constants				
F_{rr}/mdA^{-1}	=	8.454[a,b]	$F_{\theta\theta}/\text{mdA}$ =	0.699
$F_{rr'}/\text{mdA}^{-1}$	=	−0.101[a,b]	$F_{r\theta}/\text{md}$ =	0.2371[b]
F_{rrr}/mdA^{-2}	=	−59.366[a,b]	$F_{r'\theta}/\text{mdA}^{-1}$ =	−0.402[a,b]
$F_{rrr'}/\text{mdA}^{-2}$	=	0.253[a,b]	$F_{r\theta\theta}/\text{md}$ =	−0.185
$F_{rr\theta}/\text{mdA}^{-1}$	=	−0.002[b]	$F_{\theta\theta\theta}/\text{mdA}$ =	−0.6933
F_{rrrr}/mdA^{-3}	=	384.08[a,b]	$F_{rr\theta\theta}/\text{mdA}^{-1}$ =	−1.495[b]
$F_{rrrr'}/\text{mdA}^{-3}$	=	−4.96[a,b]	$F_{\theta\theta\theta\theta}/\text{mdA}$ =	−0.586
$F_{rrr'r'}/\text{mdA}^{-3}$	=	0.57[a,b]		

Molecular structure				
l_0/A	=	0.957 81[b]	θ_0/deg =	104.4776[b]

[a] Reference 1.
[b] Reference 4(b).

with the HMS force constants gave much better results than with the HB force constants. Further, our theory using the HMS force constants gave better results than the usual vibration–rotation theory using the same constants. However, as will be seen later, the HB force constants gave much better fit to the rotational data than the HMS force constants.

We have developed a set of force constants, denoted by GQ, that are much improved for the vibrational energy levels without a loss in quality for the rotational energy levels. These force constants are a further modification of the HMS force constants as first modified by HB. The HB molecular geometry is used. We found the differences in the HB and the HMS structures to play a minor role in the calculated energy levels.

The complete set of GQ force constants is given in Table I. Then the calculated and observed vibrational energy values are given in Tables II and III for those low n states for which there are experimental data based upon band origins for H_2O and D_2O.

TABLE II. This table contains the vibration–LAM energies for H_2O calculated using the Hoy–Mills–Strey, Hoy–Bunker and Guan–Quade force constants. VRT is the usual vibration–rotation theory and GQT is the present theory. Units are cm^{-1} for the energies and percent for the δ's.

Energy level	Observed	Obs − calc			
		HMS VRT	HMS GQT	HB GQT	GQ GQT
(000)	ZP	···	···	···	···
(010)	1594.7[b]	−2.5	−0.8	7.9	1.2
(020)	3156.2[a]	−4.5	−1.0	17.2	0.9
(030)	4675.2[c]	−15.4	−7.1	21.9	−7.5
(100)	3652.5[a]	−3.5	−0.8	−1.8	−2.5
(110)	5226.6[c]	−10.6	−2.3	8.8	−0.2
(001)	3755.9[a]	−1.6	−0.8	−1.1	−2.2
(011)	5331.3[c]	0.2	−2.9	11.8	2.2
δ^V	···	0.17%	0.07%	0.35%	0.08%

[a] Reference 10.
[b] Reference 11.
[c] Reference 12.

TABLE III. This table contains the vibration–LAM energies for D_2O calculated using the Hoy–Bunker and Guan–Quade force constants. All calculations were made with the present theory. Experimental data are taken from Ref. 14. Units are cm^{-1} for the energies and percent for the δ's.

Energy level	Observed	Obs − calc	
		HB	GQ
(000)	ZP	···	···
(010)	···	(1172.9)	(1176.9)
(020)	···	(2328.2)	(2337.7)
(030)	···	(3464.8)	(3481.3)
(100)	2671.7	1.0	0.6
(001)	2788.1	−1.3	−1.9
(011)	3956.2	6.9	1.3
(021)	5105.4	13.5	1.5
(200)	5291.6	−6.9	−7.7
(101)	5374.0	−1.5	−2.5
(111)	6533.4	11.2	4.5
(201)	7899.8	−18.8	−20.2
δ^V	···	0.161%	0.112%

V. THE ROTATIONAL ENERGY LEVELS

The rotational energy levels for the different vibration–LAM states are calculated by diagonalizing the matrix of the total effective rotation–LAM Hamiltonian, $H_{\tau R}^{\text{eff}}$, given by Eq. (16). This is done in the $\psi_{n_\tau JK}$ basis as defined by Eq. (26), where $\psi_{n_\tau JK}$ is a product of $\phi_{n_\tau K}$, a function of τ' and S_{JK}, an eigenfunction of a symmetric rotor. The LAM dependent parts of $H_{\tau R}^{\text{eff}}$ are numerically integrated in the $\phi_{n_\tau K}$ basis and the rotation dependent parts of $H_{\tau R}^{\text{eff}}$ are calculated in the S_{JK} basis. As an example, consider $\mu_{xx}^{\text{eff}} P_x^2$. The matrix element can be written as

$$(\psi_{n'_\tau J'K'} | \mu_{xx}^{\text{eff}} P_x^2 | \psi_{n_\tau JK})$$
$$= (\phi_{n'_\tau K'} | \mu_{xx}^{\text{eff}} | \phi_{n_\tau K})(S_{J'K'} | P_x^2 | S_{JK}) . \qquad (32)$$

The total effective LAM–rotation Hamiltonian, $H_{\tau R}^{\text{eff}}$, commutes with the total angular momentum, P^2. Therefore the matrix of $H_{\tau R}^{\text{eff}}$ is diagonal in J in the $\psi_{n_\tau JK}$ basis. For the quantum number of the component of the total angular momentum along the molecular z axis, K, it can be shown that the matrix elements of $H_{\tau R}^{\text{eff}}$ are nonzero only for $\Delta K = 0$, $\pm 2, \pm 4$ ($\Delta K = K' - K$). For the quantum number of the LAM, n_τ, there are no special selection rules for the calculation of the matrix elements of $H_{\tau R}^{\text{eff}}$. However, in general, the larger the Δn_τ ($\Delta n_\tau = n'_\tau - n_\tau$), the smaller the off-diagonal matrix elements of $H_{\tau R}^{\text{eff}}$. The off-diagonal matrix elements of $H_{\tau R}^{\text{eff}}$ are negligible when $\Delta n_\tau > 6$.

For the rotation dependent part of $H_{\tau R}^{\text{eff}}$, the matrix elements of P_x, P_y, and P_z, the components of the total angular momentum along the molecular fixed x, y, and z axes, and the products of them are well known.[9] For the LAM dependent parts of $H_{\tau R}^{\text{eff}}$, the numerical integration is done by computer. Again the error of the numerical integration is less than 10^{-7} cm^{-1}.

Our computer program can be divided into two parts—the numerical integration part and the matrix diagonalization part. To obtain the rotational energy levels for different

TABLE IV. This table contains representative rotational energy levels for H_2O using the HB and GQ force constants, calculated with the present theory. See Sec. VI for information on the HBAR and GQAR columns. The experimental data were taken from Refs. 10–13. Units are cm^{-1} for the rotational energies and percent for the δ's.

Energy	state	Observed	Obs − calc			
			HB	GQ	HBAR	GQAR
(000)	1_{01}	23.794	0.012	0.014	0.000	0.000
	1_{11}	37.137	0.049	0.036	0.000	0.000
	1_{10}	42.372	0.033	0.024	0.000	0.000
	δ_1	$\cdots$	0.093%	0.073%	0.000%	0.000%
	2_{02}	70.091	0.048	0.051	0.002	0.013
	2_{12}	79.496	0.090	0.078	0.001	0.002
	2_{11}	95.176	0.041	0.039	0.000	− 0.001
	2_{21}	134.902	0.152	0.104	0.000	− 0.002
	2_{20}	136.164	0.141	0.096	− 0.001	− 0.014
	δ_2	$\cdots$	0.093%	0.074%	0.002%	0.010%
	δ_3	$\cdots$	0.093%	0.075%	0.004%	0.020%
	δ_4	$\cdots$	0.083%	0.063%	0.021%	0.036%
	δ_5	$\cdots$	0.080%	0.060%	0.031%	0.049%
	δ_6	$\cdots$	0.078%	0.058%	0.045%	0.064%
	δ_7	$\cdots$	0.079%	0.061%	0.061%	0.080%
	δ_8	$\cdots$	0.083%	0.069%	0.081%	0.099%
	δ_9	$\cdots$	0.092%	0.081%	0.103%	0.119%
	10_{010}	1114.533	1.529	1.433	0.326	1.152
	10_{110}	1114.550	1.543	1.447	0.160	0.622
	10_{19}	1293.019	0.892	0.815	− 0.051	0.460
	10_{29}	1293.635	0.934	0.854	0.439	0.250
	10_{28}	1437.969	− 0.929	− 0.966	− 1.231	− 1.878
	10_{38}	1446.129	− 0.341	− 0.411	− 0.833	− 1.404
	10_{37}	1538.150	− 3.355	− 3.318	− 3.511	− 4.116
	10_{47}	1581.337	− 1.394	− 1.483	− 2.637	− 2.589
	10_{46}	1616.453	− 3.808	− 3.793	− 4.706	− 5.071
	10_{56}	1718.720	− 1.543	− 1.726	− 2.986	− 3.010
	10_{55}	1724.706	− 2.292	− 2.438	− 3.629	− 3.726
	10_{65}	1874.974	− 0.964	− 1.330	− 2.954	− 2.762
	10_{64}	1875.459	− 1.057	− 1.417	− 3.042	− 2.854
	10_{74}	2054.347	− 0.130	− 0.766	− 2.288	− 2.461
	10_{73}	2054.369	− 0.137	− 0.773	− 2.295	− 2.467
	10_{83}	2254.283	0.797	− 0.209	− 1.576	− 2.049
	10_{82}	2254.284	0.797	− 0.209	− 1.576	− 2.049
	10_{92}	2471.254	1.776	0.276	− 1.267	− 1.740
	10_{91}	2471.254	1.776	0.276	− 1.267	− 1.740
	$10_{10,1}$	2701.891	2.752	0.606	− 0.819	− 1.774
	$10_{10,0}$	2701.891	2.752	0.606	− 0.819	− 1.774
	δ_{10}	$\cdots$	0.104%	0.098%	0.128%	0.142%
(010)	1_{01}	23.812	− 0.015	− 0.011	0.000	0.000
	1_{11}	40.222	0.026	0.001	0.000	0.000
	1_{10}	45.761	0.018	0.002	0.000	0.000
	δ_1	$\cdots$	0.057%	0.027%	0.000%	0.000%
	2_{02}	70.223	− 0.034	− 0.029	0.012	0.004
	2_{12}	82.315	0.002	− 0.025	− 0.002	− 0.003
	2_{11}	98.905	− 0.021	− 0.021	− 0.001	− 0.002
	2_{21}	147.559	0.096	0.004	− 0.007	− 0.013
	2_{20}	148.745	0.094	0.007	− 0.010	− 0.010
	δ_2	$\cdots$	0.047%	0.025%	0.009%	0.006%
	δ_3	$\cdots$	0.043%	0.026%	0.015%	0.012%
	δ_4	$\cdots$	0.051%	0.048%	0.036%	0.035%
	δ_5	$\cdots$	0.057%	0.063%	0.051%	0.052%
	δ_6	$\cdots$	0.067%	0.079%	0.067%	0.070%
	δ_7	$\cdots$	0.083%	0.100%	0.086%	0.092%
	δ_8	$\cdots$	0.102%	0.124%	0.107%	0.117%
	δ_9	$\cdots$	0.125%	0.151%	0.131%	0.144%
	δ_{10}	$\cdots$	0.151%	0.180%	0.159%	0.174%
(020)	1_{01}	23.812	− 0.052	− 0.048	0.000	0.000
	1_{11}	44.451	0.028	0.028	0.000	0.000
	1_{10}	50.273	0.020	0.032	0.000	0.000
	δ_1	$\cdots$	0.133%	0.128%	0.000%	0.000%

TABLE IV (*continued*).

Energy	state	Observed	Obs − calc			
			HB	GQ	HBAR	GQAR
	2_{02}	70.333	− 0.143	− 0.138	0.007	0.001
	2_{12}	86.273	− 0.069	− 0.073	− 0.001	− 0.001
	2_{11}	103.707	− 0.092	− 0.062	− 0.001	− 0.002
	2_{21}	164.499	0.149	0.143	0.001	− 0.025
	2_{20}	165.564	0.138	0.136	− 0.004	− 0.027
	δ_2	⋯	0.119%	0.113%	0.004%	0.010%
	δ_3	⋯	0.111%	0.103%	0.013%	0.031%
	δ_4	⋯	0.121%	0.114%	0.044%	0.072%
	δ_5	⋯	0.126%	0.127%	0.072%	0.111%
	δ_6	⋯	0.140%	0.151%	0.105%	0.153%
	δ_7	⋯	0.162%	0.184%	0.141%	0.197%
	δ_8	⋯	0.198%	0.233%	0.191%	0.256%
(100)	1_{01}	23.400	0.017	0.020	0.000	0.000
	1_{11}	36.241	0.026	0.013	0.000	0.000
	1_{10}	41.439	0.023	0.014	0.000	0.000
	δ_1	—	0.067%	0.056%	0.000%	0.000%
	2_{02}	68.889	0.059	0.063	0.009	0.003
	2_{12}	77.844	0.060	0.048	− 0.003	− 0.004
	2_{11}	93.412	0.049	0.050	− 0.005	− 0.005
	2_{21}	131.641	0.068	0.020	− 0.013	− 0.014
	2_{20}	132.916	0.055	0.010	− 0.027	− 0.024
	δ_2	⋯	0.064%	0.055%	0.012%	0.010%
	δ_3	⋯	0.056%	0.058%	0.039%	0.038%
	δ_4	⋯	0.207%	0.187%	0.189%	0.185%
	δ_5	⋯	0.313%	0.297%	0.290%	0.287%
	δ_6	⋯	0.223%	0.209%	0.200%	0.198%
	δ_7	⋯	0.173%	0.149%	0.143%	0.137%
	δ_8	⋯	0.176%	0.147%	0.142%	0.132%
	δ_9	⋯	0.220%	0.187%	0.190%	0.178%
	δ_{10}	⋯	0.210%	0.189%	0.200%	0.192%
(110)	1_{01}	23.425	0.002	0.007	0.000	0.000
	1_{11}	39.185	− 0.007	− 0.028	0.000	0.000
	1_{10}	44.698	0.011	0.000	0.000	0.000
	δ_1	⋯	0.019%	0.045%	0.000%	0.000%
	2_{02}	69.033	0.002	0.010	0.004	0.003
	2_{12}	80.528	− 0.027	− 0.047	− 0.006	− 0.005
	2_{11}	97.038	0.029	0.037	− 0.004	− 0.005
	2_{21}	143.777	− 0.001	− 0.076	− 0.007	− 0.013
	2_{20}	144.971	− 0.011	− 0.081	− 0.025	− 0.031
	δ_2	⋯	0.020%	0.047%	0.009%	0.011%
	δ_3	⋯	0.122%	0.156%	0.124%	0.130%
	δ_4	⋯	0.278%	0.265%	0.271%	0.267%
	δ_5	⋯	0.122%	0.098%	0.120%	0.112%
	δ_6	⋯	0.118%	0.078%	0.121%	0.107%
	δ_7	⋯	0.167%	0.124%	0.172%	0.154%
	δ_8	⋯	0.223%	0.174%	0.225%	0.201%
(001)	1_{01}	23.564	0.069	0.073	0.000	0.000
	1_{11}	35.773	0.099	0.082	0.000	0.000
	1_{10}	41.052	0.042	0.031	0.000	0.000
	δ_1	⋯	0.240%	0.226%	0.000%	0.000%
	2_{02}	69.285	0.235	0.243	0.058	− 0.001
	2_{12}	77.647	0.314	0.300	0.020	0.021
	2_{11}	93.456	0.140	0.144	0.017	0.018
	2_{21}	129.808	0.222	0.159	0.009	0.006
	2_{20}	131.185	0.194	0.136	− 0.048	0.007
	δ_2	⋯	0.266%	0.254%	0.043%	0.015%
	δ_3	⋯	0.299%	0.286%	0.085%	0.063%
	δ_4	⋯	0.332%	0.330%	0.237%	0.239%
	δ_5	⋯	0.387%	0.384%	0.368%	0.379%
	δ_6	⋯	0.284%	0.277%	0.273%	0.246%
	δ_7	⋯	0.240%	0.229%	0.214%	0.197%
	δ_8	⋯	0.239%	0.227%	0.220%	0.212%
	δ_9	⋯	0.259%	0.247%	0.258%	0.252%

TABLE IV (*continued*).

Energy	state	Observed	Obs — calc			
			HB	GQ	HBAR	GQAR
	δ_{10}	⋯	0.243%	0.232%	0.223%	0.228%
(011)	1_{01}	23.602	0.057	0.065	0.000	0.000
	1_{11}	38.486	− 0.013	− 0.043	0.000	0.000
	1_{10}	44.088	− 0.050	− 0.068	0.000	0.000
	δ_1	⋯	0.156%	0.193%	0.000%	0.000%
	2_{02}	69.466	0.185	0.199	0.037	0.001
	2_{12}	80.132	0.171	0.145	0.033	0.033
	2_{11}	96.894	0.046	0.057	0.019	0.020
	2_{21}	141.066	− 0.151	− 0.260	0.032	0.027
	2_{20}	142.372	− 0.164	− 0.264	− 0.004	0.026
	δ_2	⋯	0.169%	0.193%	0.033%	0.024%
	δ_3	⋯	0.278%	0.279%	0.210%	0.212%
	δ_4	⋯	0.407%	0.416%	0.390%	0.388%
	δ_5	⋯	0.193%	0.221%	0.162%	0.142%
	δ_6	⋯	0.193%	0.220%	0.158%	0.128%
	δ_7	⋯	0.237%	0.257%	0.213%	0.188%
	δ_8	⋯	0.201%	0.230%	0.150%	0.124%
	δ_9	⋯	0.213%	0.241%	0.170%	0.151%
	δ_{10}	⋯	0.238%	0.266%	0.203%	0.190%
	δ^R_{total}	⋯	0.1898%	0.1887%	0.1669%	0.1671%

vibration–LAM states, first, $H^{\text{eff}}_{\tau R}(1)$ in Eq. (24a) is numerical integrated in the Fourier sine basis. Diagonalization of the matrix of $H^{\text{eff}}_{\tau R}(1)$ yields $E_{n_\tau K}(1)$, the eigenenergies of $H^{\text{eff}}_{\tau R}(1)$, and $\phi_{n_\tau K}$, the eigenfunctions of $H^{\text{eff}}_{\tau R}(1)$ which are used as the basis functions for the total effective rotation–LAM Hamiltonian, $H^{\text{eff}}_{\tau R}$. Second, $H^{\text{eff}}_{\tau R}$ is numerical integrated in the $\psi_{n_\tau JK}$ basis in which $H^{\text{eff}}_{\tau R}(1)$ is diagonal. Then diagonalization of the matrix of $H^{\text{eff}}_{\tau R}$ yields the desired rotational energy levels. Since $H^{\text{eff}}_{\tau R}(1)$ is diagonal in this basis, K is a good quantum number for the "eigenstates" of $H^{\text{eff}}_{\tau R}(1)$. However, $H^{\text{eff}}_{\tau R}$ is diagonal in neither K nor n_τ. Therefore K is not a good quantum number for the eigenstates of $H^{\text{eff}}_{\tau R}$, the total effective rotation–LAM Hamiltonian. To summarize, the procedure of numerical integration–matrix diagonalization is used twice to calculate the rotational eigenenergies.

The results of our calculations of the rotational energy levels are given in Tables IV and V for H_2O and D_2O, respectively. To estimate the quality of each calculation, the quantity δ, defined by

$$\delta = \left\{ \Sigma \frac{1}{N} \left(\frac{\text{obs} - \text{calc}}{\text{obs}} \right)^2 \right\}^{1/2}, \qquad (33)$$

is used where N is the total numer of rotational states. For H_2O we used $J = 1$ to 10 for (000), (010), (001), and (011); $J = 1$ to 8 for (020) and (110). The states for $10_{10,0}$ and $10_{10,1}$ were not included in δ analysis for the (010) state. For D_2O we used $J = 1$ to 10 for (000); $J = 1$ to 3 for (010); $J = 1$ to 7 for (100); $J = 1$ to 8 for (001); $J = 1$ to 6 for (011); and $J = 1$ to 5 for (021) in δ analysis.

For the purpose of a force constant comparison, we have given partial δ_J's. Only a representative listing is given of the

energy levels in Tables IV and V. But the summary δ_{total} is given for all of the energy levels in the previous paragraph.

Although there is a clear cut difference in the calculated rotational energy levels using the HB and GQ force constants, δ^R_{HB} is essentially the same as δ^R_{GQ}. On the other hand, δ^v_{GQ} is substantially improved over δ^v_{HB}. Rotational calculations were also made using the HMS constants, but these results were very, very poor when compared with either the results from HB or GQ force constants and are not tabulated here.

VI. DISCUSSION

In this section we discuss some of the quantitative and qualitative features of the theory as applied to water in the calculation of vibration–rotation–LAM energy levels. Certain results suggest an extension of the theory as long as a computer is not available to crunch things out without series expansions, coordinate transformations, and Van Vleck transformation. This situation applies to, and is limited to, the calculation of the energy levels of water.

A. Limitations of the theory

While the theory is rigorous in its diagonalization of the effective LAM–rotation Hamiltonian, the theory does not include: (1) terms beyond quadratic in the small amplitude coordinate (SAC) dependence of the moments of inertia and Coriolis coupling coefficients; (2) an n^2_k dependence in the SAC dependence of the rotational coefficients; and (3) sextic and higher order centrifugal distortion effects in the SAMs and their interaction with the LAM. At the same time, it should be noted that nonasymmetric rotor terms appear from the diagonalization of the rotation–LAM effec-

TABLE V. This table contains representative rotational energy levels for D_2O using the HB and GQ force constants, calculated with the present theory. See Sec. VI for information on the HBAR and GQAR columns. The experimental data were taken from Refs. 14 and 15. Units are cm^{-1} for the rotational energies and percent for δ's.

| | | | Obs − calc | | | |
Energy	state	Observed	HB	GQ	HBAR	GQAR
(000)	1_{01}	12.117	0.002	0.003	0.001	0.000
	1_{11}	20.259	0.013	0.007	0.000	0.000
	1_{10}	22.684	0.006	0.002	0.000	0.000
	δ_1	...	0.041%	0.025%	0.006%	0.000%
	2_{02}	35.878	0.010	0.011	0.009	0.004
	2_{12}	42.069	0.023	0.018	0.001	0.000
	2_{11}	49.339	0.004	0.003	0.003	0.000
	2_{21}	73.676	0.035	0.014	− 0.002	− 0.001
	2_{20}	74.142	0.033	0.012	− 0.007	− 0.005
	δ_2	...	0.040%	0.026%	0.013%	0.006%
	δ_3	...	0.041%	0.027%	0.020%	0.013%
	δ_4	...	0.037%	0.024%	0.027%	0.022%
	δ_5	...	0.036%	0.025%	0.035%	0.031%
	δ_6	...	0.037%	0.029%	0.044%	0.040%
	δ_7	...	0.041%	0.036%	0.054%	0.051%
	δ_8	...	0.048%	0.045%	0.065%	0.063%
	δ_9	...	0.057%	0.057%	0.077%	0.077%
	10_{010}	581.819	0.367	0.337	0.592	0.383
	10_{110}	581.844	0.371	0.341	0.271	0.154
	10_{19}	672.914	0.010	− 0.010	0.217	0.038
	10_{29}	673.711	0.049	0.026	0.067	− 0.058
	10_{28}	743.795	− 0.738	− 0.730	− 0.943	− 0.971
	10_{38}	752.601	− 0.395	− 0.414	− 0.577	− 0.630
	10_{37}	790.810	− 1.394	− 1.363	− 1.493	− 1.534
	10_{47}	826.181	− 0.658	− 0.695	− 1.044	− 1.026
	10_{46}	837.036	− 1.234	− 1.238	− 1.678	− 1.622
	10_{56}	906.921	− 0.615	− 0.702	− 0.942	− 1.021
	10_{55}	908.188	− 0.726	− 0.807	− 1.058	− 1.129
	10_{65}	1002.771	− 0.413	− 0.579	− 0.724	− 0.767
	10_{64}	1002.845	− 0.422	− 0.588	− 0.733	− 0.776
	10_{74}	1114.844	− 0.182	− 0.455	− 0.718	− 0.644
	10_{73}	1114.847	− 0.181	− 0.455	− 0.718	− 0.644
	10_{83}	1241.934	− 0.532	− 0.359	− 0.514	− 0.591
	10_{82}	1241.934	− 0.532	− 0.359	− 0.514	− 0.591
	10_{92}	1382.689	0.282	− 0.307	− 0.442	− 0.605
	10_{91}	1382.689	0.282	− 0.307	− 0.442	− 0.605
	10_{101}	1535.839	0.494	− 0.319	− 0.405	− 0.637
	10_{100}	1535.839	0.494	− 0.319	− 0.405	− 0.637
	δ_{10}	...	0.068%	0.070%	0.092%	0.092%
	$\delta_{subtotal}$	...	0.049%	0.046%	0.062%	0.060%
(010)	1_{01}	12.129	− 0.007	− 0.006	0.000	0.000
	1_{11}	21.417	0.009	− 0.004	− 0.001	0.000
	1_{10}	23.962	0.006	− 0.004	− 0.001	0.000
	δ_1	...	0.044%	0.030%	0.004%	0.000%
	2_{02}	35.923	− 0.020	− 0.018	0.001	0.000
	2_{12}	43.132	− 0.003	− 0.016	− 0.002	0.000
	2_{11}	50.761	− 0.011	− 0.015	− 0.001	0.001
	2_{21}	78.485	0.036	− 0.012	− 0.005	− 0.002
	2_{20}	78.940	0.034	− 0.012	− 0.007	− 0.002
	δ_2	...	0.039%	0.032%	0.006%	0.002%
	δ_3	...	0.037%	0.033%	0.010%	0.005%
	$\delta_{subtotal}$	...	0.039%	0.032%	0.008%	0.004%
(100)	1_{01}	11.980	0.024	0.025	...	...
	1_{11}	19.980	0.012	0.006	...	...
	1_{10}	22.350	− 0.020	− 0.025	...	...
	δ_1	...	0.131%	0.140%	...	...
	2_{02}	35.300	− 0.096	− 0.093	...	...
	2_{12}	41.360	− 0.118	− 0.124	...	...
	2_{11}	48.580	− 0.100	− 0.101	...	...
	2_{21}	72.570	− 0.058	− 0.083	...	...
	2_{20}	73.060	− 0.032	− 0.056	...	...
	δ_2	...	0.203%	0.210%	...	...
	δ_3	...	0.151%	0.151%	...	...

TABLE V (continued).

| Energy | state | Observed | Obs − calc | | | |
			HB	GQ	HBAR	GQAR
	δ_4	⋯	0.085%	0.090%	⋯	⋯
	δ_5	⋯	0.112%	0.113%	⋯	⋯
	δ_6	⋯	0.132%	0.150%	⋯	⋯
	δ_7	⋯	0.353%	0.376%	⋯	⋯
(001)	1_{01}	12.000	− 0.016	− 0.015	⋯	⋯
	1_{11}	19.580	− 0.068	− 0.076	⋯	⋯
	1_{10}	22.030	− 0.089	− 0.094	⋯	⋯
	δ_1	⋯	0.318%	0.340%	⋯	⋯
	2_{02}	35.530	− 0.002	0.001	⋯	⋯
	2_{12}	41.280	0.068	0.062	⋯	⋯
	2_{11}	48.620	0.003	0.003	⋯	⋯
	2_{21}	71.310	− 0.123	− 0.151	⋯	⋯
	2_{20}	71.860	− 0.082	− 0.108	⋯	⋯
	δ_2	⋯	0.119%	0.134%	⋯	⋯
	δ_3	⋯	0.066%	0.053%	⋯	⋯
	δ_4	⋯	0.042%	0.058%	⋯	⋯
	δ_5	⋯	0.116%	0.105%	⋯	⋯
	δ_6	⋯	0.208%	0.198%	⋯	⋯
	δ_7	⋯	0.447%	0.431%	⋯	⋯
	δ_8	⋯	0.378%	0.368%	⋯	⋯
(011)	1_{01}	12.020	− 0.019	− 0.017	⋯	⋯
	1_{11}	20.670	− 0.054	− 0.069	⋯	⋯
	1_{10}	23.200	− 0.114	− 0.124	⋯	⋯
	δ_1	⋯	0.333%	0.373%	⋯	⋯
	2_{02}	35.520	− 0.092	− 0.086	⋯	⋯
	2_{12}	42.120	− 0.096	− 0.110	⋯	⋯
	2_{11}	49.820	− 0.157	− 0.157	⋯	⋯
	2_{21}	75.670	− 0.238	− 0.292	⋯	⋯
	2_{20}	76.180	− 0.225	− 0.277	⋯	⋯
	δ_2	⋯	0.284%	0.319%	⋯	⋯
	δ_3	⋯	0.124%	0.167%	⋯	⋯
	δ_4	⋯	0.134%	0.166%	⋯	⋯
	δ_5	⋯	0.101%	0.139%	⋯	⋯
	δ_6	⋯	0.095%	0.108%	⋯	⋯
(021)	1_{01}	12.040	− 0.021	− 0.017	⋯	⋯
	1_{11}	22.050	0.002	− 0.017	⋯	⋯
	1_{10}	24.670	− 0.083	− 0.093	⋯	⋯
	δ_1	⋯	0.219%	0.237%	⋯	⋯
	2_{02}	35.750	0.056	0.064	⋯	⋯
	2_{12}	43.320	− 0.149	− 0.164	⋯	⋯
	2_{11}	51.570	− 0.006	− 0.003	⋯	⋯
	2_{21}	81.060	− 0.282	− 0.341	⋯	⋯
	2_{20}	81.450	− 0.371	− 0.427	⋯	⋯
	δ_2	⋯	0.307%	0.354%	⋯	⋯
	δ_3	⋯	0.297%	0.330%	⋯	⋯
	δ_4	⋯	0.232%	0.276%	⋯	⋯
	δ_5	⋯	0.324%	0.364%	⋯	⋯
	δ_{Total}^R	⋯	0.195%	0.204%	⋯	⋯

tive Hamiltonian. These terms cannot be accounted for by an effective asymmetric rotor Hamiltonian and are significant for H_2O.

B. Asymmetric rotor and centrifugal distortion effects in the observed minus calculated results

Every vibrational state shows very clearly "asymmetric rotor" differences for low J. By introducing asymmetric ro-tor corrections for each vibrational state, the obs–calc differences can be made essentially zero for low J. Calculations performed in this manner are denoted by HBAR and GQAR. The ΔA, ΔB, ΔC for each vibrational state are given in Tables VI and VII. Algebraic equations have been developed that depend upon the cubic anharmonicities to see if this asymmetric rotor effect could be removed by changing the force constants. The GQ force constants come from a partially successful attempt at this. However, it is clear from

TABLE VI. This table contains the asymmetric rotor corrections for H_2O that are present in the obs − calc differences using both the HB and GQ force constants. These terms cannot be accounted for with the present theory and force constants. Each $\Delta A, \Delta B, \Delta C$ is added to the respective calculation to make obs − calc small for low J. Units are cm^{-1}.

Energy level	HBAR	GQAR
(000)	$\Delta A =$ 0.035	$\Delta A =$ 0.023
	$\Delta B = -$ 0.002	$\Delta B =$ 0.001
	$\Delta C =$ 0.014	$\Delta C =$ 0.013
(010)	$\Delta A =$ 0.029	$\Delta A =$ 0.007
	$\Delta B = -$ 0.011	$\Delta B = -$ 0.005
	$\Delta C = -$ 0.003	$\Delta C = -$ 0.006
(020)	$\Delta A =$ 0.050	$\Delta A =$ 0.054
	$\Delta B = -$ 0.030	$\Delta B = -$ 0.022
	$\Delta C = -$ 0.022	$\Delta C = -$ 0.026
(100)	$\Delta A =$ 0.016	$\Delta A =$ 0.003
	$\Delta B =$ 0.007	$\Delta B =$ 0.011
	$\Delta C =$ 0.010	$\Delta C =$ 0.009
(110)	$\Delta A =$ 0.001	$\Delta A = -$ 0.018
	$\Delta B =$ 0.010	$\Delta B =$ 0.018
	$\Delta C = -$ 0.008	$\Delta C = -$ 0.011
(001)	$\Delta A =$ 0.036	$\Delta A =$ 0.020
	$\Delta B =$ 0.006	$\Delta B =$ 0.011
	$\Delta C =$ 0.063	$\Delta C =$ 0.062
(011)	$\Delta A = -$ 0.060	$\Delta A = -$ 0.088
	$\Delta B =$ 0.010	$\Delta B =$ 0.020
	$\Delta C =$ 0.047	$\Delta C =$ 0.045

the algebraic equations that within our theory these asymmetric rotor residual effects cannot be completely removed. Our suspicion is that these differences arise from higher order effects in the theory such as would appear as n_k^2 or $n_r n_k$ dependence in the rotational coefficients in the usual vibration–rotation theory.

At the same time, while the GQ force constants and asymmetric rotor additions work much better for low J, things are made worse for high J. This suggests that higher order centrifugal distortion effects, which are not included in our theory for the LAM, are significant. It is well established that H_K, H_{JK}, and h_K are large for H_2O.[16] But without an extended theory it is not possible to isolate the LAM and SAM contributions to the centrifugal distortion effects.

TABLE VII. This table contains the asymmetric rotor corrections for the (000) and (010) states of D_2O that are present in the obs − calc differences using the HB and GQ force constants. The (100), (001), (011), and (021) states do not show this behavior. Units are cm^{-1}.

Energy level	HBAR	GQAR
(000)	$\Delta A =$ 0.009	$\Delta A =$ 0.003
	$\Delta B = -$ 0.003	$\Delta B = -$ 0.001
	$\Delta C =$ 0.004	$\Delta C =$ 0.004
(010)	$\Delta A =$ 0.012	$\Delta A = -$ 0.001
	$\Delta B = -$ 0.005	$\Delta B = -$ 0.003
	$\Delta C = -$ 0.002	$\Delta C = -$ 0.003

Therefore, using either the HB or GQ force constants, the asymmetric rotor "errors" are in direct competition with, and are compensating for, the centrifugal distortion errors.

C. Higher order Van Vleck contributions

In the vibration–LAM interaction, we have taken the Van Vleck perturbation through fourth order. In the vibration–rotation interaction, we have taken the Van Vleck perturbation through second order. To see if the third order terms in the vibration–rotation interaction could account for the asymmetric rotor discrepancies as observed in the analysis, the leading terms that arise in the third order were investigated. These terms contribute at most 1% to the observed calc − obs differences. There are also fourth order terms that are asymmetric rotor in behavior, but the size of these terms was not investigated.

D. Changes in the force constants

The calculated vibrational energy levels were improved by changes in $F_{\theta\theta}$, $F_{\theta\theta\theta}$, and $F_{\theta\theta\theta\theta}$. The $F_{\theta\theta}$ and $F_{\theta\theta\theta\theta}$ changes made the rotational calculations worse for low J while both $F_{\theta\theta r}$ and $F_{\theta\theta\theta}$ made them better. The pure stretching constants, F_{rrrr}, etc., were varied which improved the vibrational calculations for n_+ and n_- excited states but had an adverse effect on the rotational calculations for the excited n_r states. However, since the force constants are underdetermined to the extent of our calculation, we continued to use the HMS constants for the stretching modes. At the same time, other force constants were varied, but without well-defined success.

E. Results for D_2O

Although, to the order taken in the theoretical calculation, things should work equally well for H_2O and D_2O, the results for D_2O are interesting but not helpful for a complete force constant analysis due to a lack of experimental data. Even so, the same qualitative conclusions apply as were deduced from the H_2O analysis: The GQ force constants are better for the vibrational energy levels, especially those associated with the LAM. But the rotational analysis for D_2O suggests that the GQ force constants work best for the pure bending modes while the HB force constants work best for the excited stretching modes. However, as indicated in the next paragraph, these stretching modes show an unusual behavior when compared to all other results of this calculation.

There remains a significant asymmetric rotor contribution to the obs − calc differences for only the (000) and (010) vibrational states. For those states with an excited stretching mode—(100), (001), (011), (021)—the obs − calc differences for the low J are not asymmetric rotor in behavior. At this point we have no reason to question the quality of our calculation. At the same time we have no reason to question the quality of the spectroscopic data. We do consider it unusual that all vibrational levels for H_2O have asymmetric rotor obs − calc differences while only the pure bending levels for D_2O show this feature. Even so, there also remain unaccounted for the centrifugal effects at high J states for D_2O.

These calculations for water demonstrate that the curvilinear coordinate approach to vibration–rotation–LAM interactions is not only applicable, but also useful. The "new" GQ force constants work well for both the vibrational and rotational energy levels. At the same time, the typical 0.1% difference between observed and calculated rotational energy levels clearly demonstrate the inadequacy or incompleteness of the present theoretical model with respect to higher order contributions that are necessary to completely understand the water spectra.

Three things are suggested by these results. First, the power series expansion of the potential energy may not be adequate for the bending mode. Second, theoretical sextic centrifugal distortion coefficients for the SAMs are needed to understand the high J rotational energy states. Third, and most difficult, n_k^2 and $n_k n_r$ terms are needed for the rotational coefficients. (At the same time that the present theory undergoes expansion, there may very well be value in the brute force approach of setting up the energy matrix in an appropriate basis without series expansions nor coordinate transformations for as high J as possible.) Further, more spectroscopic data are needed for both H_2O and D_2O to perform the desired potential energy determination in order to arrive at a unique set of force constants. Substantial progress can be made in this direction with the present theory with the additional experimental data.

In conclusion we make a more detailed comparison of the approach of the present work with that of Hougen, Bunker, and Johns[3] as extended by Hoy and Bunker[4(d)] and most recently by Jensen and Bunker.[17, 18(a), 18(b)] First, the Jensen-extended HBJ theory is limited in its application to triatomic molecules but these molecules may have either asymmetric or symmetric forms. The Guan–Quade theory, while applicable to other types of systems than triatomic molecules with a LAM, at present has only been developed for molecules where the orientation of the principal axes in zeroth order in the SAMs does not change with the LAM. For example, we can only do calculations with the present theory for H_2O and D_2O not for HDO. Likewise, our theory is suitable for vibration–rotation–internal rotation interactions in CH_3OH, CD_3OH, etc., but not for CH_2DOH, etc.

Second, both theories are equally rigorous in their basic formalisms but there are differing approximations in solution. In both approaches all vibrations are first separated from rotation in zeroth order and then the bending mode is separated from the stretching modes, likewise in zeroth order, in the kinetic energy. However, the following differences should be noted: (1) rectilinear Cartesian coordinates were used in the extended HBJ theory while curvilinear internal coordinate were used in the present work for the vibrational degrees of freedom; and (2) traditional Sayvetz–Eckart conditions were used for the separations in the extended HBJ theory while the R and T transformations were used in the present work. These latter transformations were developed specifically so that the curvilinear internal coordinates could be used for the vibrational degrees of freedom. The T transformation has been shown to be equivalent to the Eckart conditions.[19] However, since the choice of the Sayvetz condition is not unique, even for one particular mole-

cule, the extended HBJ "Sayvetz condition" cannot be readily identified with and compared with our R transformation. (This means that our τ' is *not* the same as the effective bending coordinate of the extended HBJ theory.) Even so, the effective zeroth order kinetic energy coefficient is the same in both theories. The differences are in the coordinate dependence of $G'_{\tau\tau}$ and the $G'_{t\tau}$, generally a second order effect. Whether one separation method is clearly better than the other can only be demonstrated from a comparison of the size of the perturbation terms.

Third, the vibrational bases for the two alternative theories are different. In the extended HBJ theory, the harmonic vibrational frequencies for the SAMs are LAC dependent. Additional terms are introduced into the Hamiltonian to handle this. In the present work, the formalism is developed in such a way that the harmonic frequencies are LAC independent. The LAC dependence of the G and F matrices is taken as part of the interaction perturbation. Our approach deletes some singularities in the Hamiltonian which would be caused by LAC dependent harmonic stretching frequencies. This is another feature that makes quantitative comparison of the intermediate stages impossible.

Fourth, the extended HBJ theory uses a power series in the LAC (bending coordinate) as the basis functions for H_τ. Our approach uses Fourier sine series for the basis of H_τ. As discussed earlier in the text, the use of Fourier sine series makes it simple and natural to remove the remaining singularities in the Hamiltonian when it is put into Hermitian form. The result is that numerical integration of the effective Hamiltonian for the extended HBJ theory and the present theory were computed in two different sets of basis functions for the LAM.

Fifth, other than the different definitions of the ω_v's, the second order treatment of the Hamiltonian to isolate an effective $H_{\tau R}$ is essentially the same in the two approaches. However, the extended HBJ theory introduces "denominator corrections" from E_τ and E_R into the "second order" energy differences that normally would depend only upon E_v. On the other hand, the present theory, without further approximation, takes the LAM–SAM interaction to fourth order in the Van Vleck transformation. Further, the third order terms in the LAM–SAM–ROT interaction have been calculated. As noted previously in the text, these terms are of the order of 1% of the obs – calc energy differences. It is well known that denominator corrections are only a portion of the third order corrections.[20] And a third order Van Vleck transformation in operator form is necessary to pick up the contributions from the asymmetry of the molecule. These latter terms do not appear to be included in the extended HBJ theory.

Finally, a comparison of the calculated results is in order. Using the Hoy–Bunker force constants, our calculated vibrational and rotational term values are comparable to those of Jensen, Bunker et al.[18(b),21] for H_2O and D_2O. Since these investigators find their denominator corrections consequential and we find our third order LAM–VIB–ROT contributions to be inconsequential except for the VIB–LAM interaction, it is suggested that the present theory is more accurate in lower order approximation than the ex-

tended HBJ theory. This can occur from any one of four places in the calculations: (1) the R transformation is better than the Sayvetz condition(s) for the VIB–LAM separation; (2) the use of a LAM independent normal coordinate treatment for the vibrations is a better approximation; (3) the Fourier sine basis for the LAM may be preferable; and/or (4) the rigorous third and fourth order treatment of the LAM–VIB interaction is better than the denominator correction approach.

In any case, the extended HBJ theory is ready for application to triatomic molecules of lower symmetry than H_2O while the present theory is ready for application to larger molecules subject to the restrictions stated above. Further, for H_2O it is clear that both approaches need Hamiltonians that are higher order in the basic contributions in order to improve upon the present obs — calc results. These basic interactions would include, but not necessarily be limited to, (1) higher order than quartic centrifugal distortion and (2) cubic and quartic terms in the expanded form of the rotational coefficients.

ACKNOWLEDGMENT

[1] A. R. Hoy, I. M. Mills, and G. Strey, Mol. Phys. **24**, 1265 (1972).

[2] C. R. Quade, J. Chem. Phys. **64**, 2783 (1976).

[3] J. T. Hougen, P. R. Bunker, and J. W. C. Johns, J. Mol. Spectrosc. **34**, 136 (1970).

[4] (a) P. R. Bunker and J. M. R. Stone, J. Mol. Spectrosc. **41**, 310 (1972); (b) A. R. Hoy and P. R. Bunker, ibid. **52**, 439 (1974); (c) P. R. Bunker and B. M. Landsberg, ibid. **67**, 374 (1977); (d) A. R. Hoy and P. R. Bunker, ibid. **74**, 1 (1979).

[5] R. J. Whitehead and N. C. Handy, J. Mol. Spectrosc. **55**, 356 (1975).

[6] C. L. Chen, B. Maessen, and M. Wolfsberg, J. Chem. Phys. **83**, 1795 (1985).

[7] Y. Guan and C. R. Quade, J. Chem. Phys. **84**, 5624 (1986).

[8] See, for example, H. H. Nielsen, Rev. Mod. Phys. **23**, 90 (1951).

[9] See, for example, W. Gordy and R. L. Cook, Microwave Molecular Spectra (Wiley, New York, 1970).

[10] J. M. Flaud and C. Camy-Peyret, J. Mol. Spectrosc. **51**, 142 (1974).

[11] C. Camy-Peyret and J. M. Flaud, Mol. Phys. **32**, 523 (1976).

[12] C. Camy-Peyret and J. M. Flaud, J. Mol. Spectrosc. **59**, 327 (1976).

[13] J. M. Flaud and C. Camy-Peyret, Mol. Phys. **32**, 499 (1976).

[14] W. S. Benedict, N. Gailar, and E. K. Plyler, J. Chem. Phys. **24**, 1139 (1956).

[15] G. Steenbeckeliers and J. Bellet, J. Mol. Spectrosc. **45**, 10 (1973).

[16] J. K. Messer and F. C. De Lucia, Int. J. Infrared Milling Waves **4**, 505 (1983).

[17] P. Jensen, Comp. Phys. Rep. **1**, 1(1983).

[18] (a) P. Jensen and P. R. Bunker, J. Mol. Spectrosc. **118**, 18 (1986); (b) R. Beardsworth, P. R. Bunker, P. Jensen, and W. P. Kraemer, ibid. **118**, 50(1986).

[19] C. R. Quade, J. Chem. Phys. **82**, 2509(1985).

[20] (a) E. U. Condon and G. H. Shortley, The Theory of Atomic Spectra (Cambridge University, Cambridge, MA, 1957), p. 34; (b) C. R. Quade, J. Chem. Phys. **47**, 1073 (1967).

[21] P. R. Bunker (private communication).